

NANO EXPRESS

Open Access



Focused Role of an Organic Small-Molecule PBD on Performance of the Bistable Resistive Switching

Lei Li¹, Yanmei Sun¹, Chunpeng Ai¹, Junguo Lu¹, Dianzhong Wen^{1*} and Xuduo Bai^{2*}

Abstract

An undoped organic small-molecule 2-(4-tert-butylphenyl)-5-(4-biphenyl)-1,3,4-oxadiazole (PBD) and a kind of nanocomposite blending poly(methyl methacrylate) (PMMA) into PBD are employed to implement bistable resistive switching. For the bistable resistive switching indium tin oxide (ITO)/PBD/Al, its ON/OFF current ratio can touch 6. What is more, the ON/OFF current ratio, approaching to 10^4 , is available due to the storage layer PBD:PMMA with the chemical composition 1:1 in the bistable resistive switching ITO/PBD:PMMA/Al. The capacity, data retention of more than 1 year and endurance performance ($>10^4$ cycles) of ITO/PBD:PMMA(1:1)/Al, exhibits better stability and reliability of the samples, which underpins the technique and application of organic nonvolatile memory.

Keywords: ITO/PBD/Al, Small molecule, PBD:PMMA nanocomposite film, Nonvolatile bistable resistive switching

Background

Organic memory, a multidisciplinary and flourishing frontier of nanotechnology, has succeeded in significant breakthroughs [1–4]. As emerging information medium, devices function as the transmission and manipulation of data, based on organic semiconductor embracing small molecule and polymer. In contrast to inorganic resistive random access memory [5–8], organic resistive random access memory (ORRAM) obtains access to meet the requirements of data storage, large-scale, low-cost, flexible nonvolatile storage for commercialization and utility.

1,3,4-oxadiazole and its derivatives are the group of electron-transport luminescent materials in the domain of organic light emitting diodes (OLEDs). The organic small-molecule material, 2-(4-tert-butylphenyl)-5-(4-biphenyl)-1,3,4-oxadiazole (PBD), predominantly emits either blue or purple light, offsetting the deficiency of blue or purple luminescent materials [9]. Nonvolatile memory on 1,3,4-oxadiazoles acting as an electron-acceptor mainly focuses on donor-acceptor (D-A) copolymers [10–12]. Transparent

material, poly(methyl methacrylate) (PMMA), is used to manufacture various illuminant equipments, optical glass, and optical fiber. For ORRAM, inorganic materials as reported cover quantum dots [13, 14], such as CuInS₂-ZnS core-shell quantum dots and thiol-capped CdS quantum dots, oxide nanoparticles (NPs) ZnO [15], and carbon nanomaterials like graphene, CNTs, and fullerene together with its derivatives [16–21], which can be embedded into the insulator-like matrix PMMA.

Not only single organic materials, such as poly(N-vinylcarbazole) (PVK) that is widely accepted, but nanocomposites with polymer-polymer or polymer-inorganic blending have unfolded for the research on organic memory. Progressively, ORRAM based on small molecule is attached to great importance. The spin-coated PBD and PBD:PMMA nanocomposite film, first and foremost, were characterized by means of Raman spectrum, scanning electron microscope (SEM), UV-Vis spectroscopy, cyclic voltammetry (CV), and transmission electron microscopy (TEM). The following work highlights the tunable effect of the organic material PBD and its nanocomposite blended by PMMA on electrical properties, and retention and endurance of the resistive switching were additionally detected.

* Correspondence: wendianzhong@hlju.edu.cn; xuduobai@hotmail.com

¹HLJ Province Key Laboratories of Senior-education for Electronic Engineering, Heilongjiang University, Harbin 150080, China

²School of Chemistry and Materials Science, Heilongjiang University, Harbin 150080, China

Methods

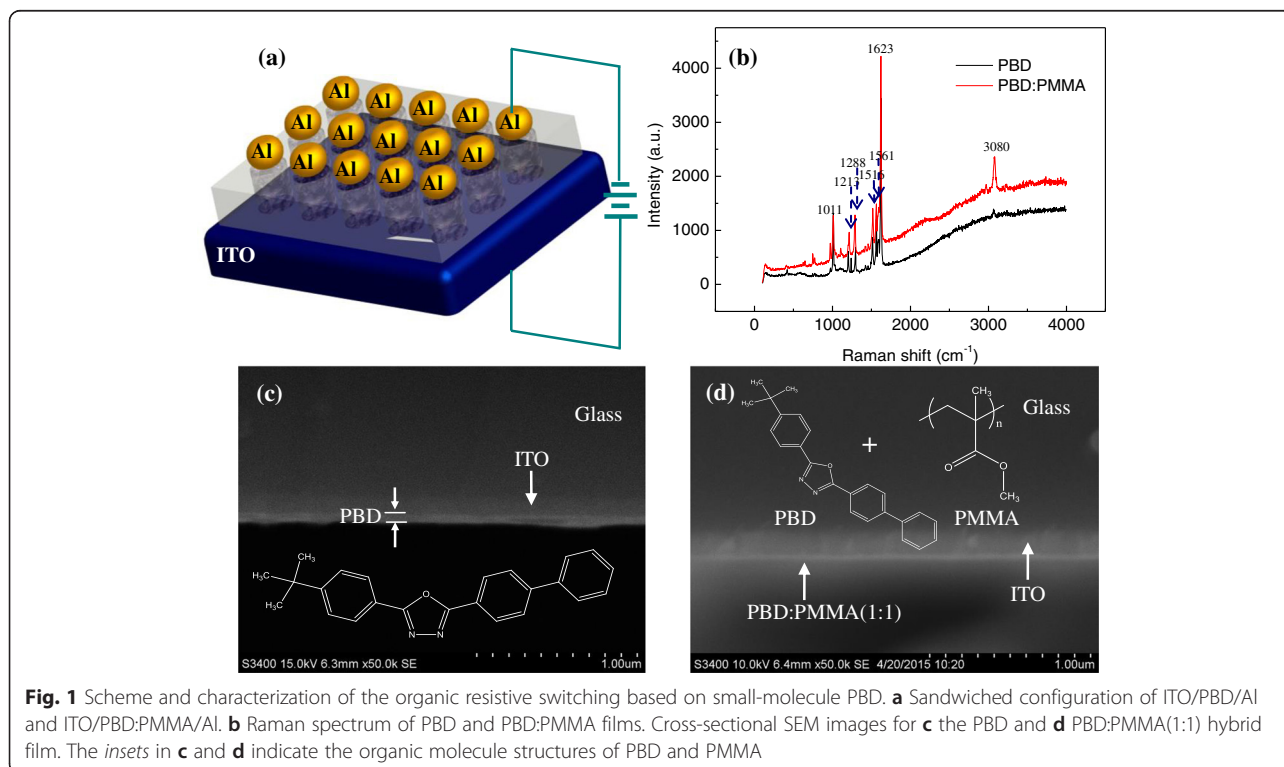
2-(4-tert-butylphenyl)-5-(4-biphenyl)-1,3,4-oxadiazole or PBD:PMMA blends with proportionality of the chemical composition 1:1 was dissolved into the chloroform with the concentration of 0.5 wt.%. At ambient temperature, the solution was stirred by the magnetic stirrer for more than 24 h. Impurities were then removed by the percolation of a 0.45- μm filter. The glass substrate, with the indium tin oxide (ITO, 2000 Å thick) deposited, was sequentially cleaned by the acetone, methanol, and ethanol and proceeded to be kept 40 °C in the vacuum furnace for 30 min. After spin-coating the solution uniformly to fabricate an active layer at 3000 rpm, the solvent was eliminated from the coatings through the vacuum furnace in 70 °C for 2 h. Later, the top aluminum electrode, 300 nm thick, was deposited on the PBD or PBD:PMMA hybrid film and protected by the mask layer with the mask pattern diameter 2 mm. The ITO electrode acts as the anode while the alternative can be seen as the cathode.

Results and Discussion

The sandwiched configuration of both ITO/PBD/Al and ITO/PBD:PMMA/Al is illustrated in Fig. 1a. As shown in Fig. 1b, Horiba Jobin Yvon LabRam HR800 Raman spectroscopy was adopted to test the Raman spectrum of the PBD film and the PBD:PMMA with the ratio of the chemical composite 1:1 coated on the ITO substrate. For the PBD film and PBD:PMMA nanocomposites, the maximum peak is located in 1625 and 1623 cm^{-1} ,

respectively, which is derived from the C–C stretching vibration of the aromatic ring. The rocking vibration peak for the hydrogen atoms on the benzene ring ranges from 500 to 900 cm^{-1} , which bears the weak Raman activity. Owing to the C–O–C stretching mode of the 1,3,4-oxadiazole ring, the obvious peak is in 1011 cm^{-1} . Ranging between 1514 and 1625 cm^{-1} , the stronger Raman activity can be found in that it has the C–C stretching pattern in the benzene ring. Besides, the peak of the C–H asymmetrical stretching vibration in the methyl for the PBD and PBD:PMMA hybrid film is separately 3074 and 3080 cm^{-1} , which has the weak Raman activity. Therefore, the stretching culmination, compared with the Raman spectrum of the undoped PBD film, can be boosted by blending PMMA. The cross sections of the undoped PBD nanofilm and doped PBD:PMMA(1:1) nanocomposite film below 50 nm were characterized by xHITACHI S3400-N scanning electron microscope (SEM), exhibited in Fig. 1c, d. Apart from that, Nano-Map 500LS Profilometer (aep Technology) was used to measure the thickness of the manufactured PBD as well as PBD:PMMA(1:1) hybrid film. It is shown that a 45.7-nm-thick PBD film was spin coated while the PBD:PMMA(1:1) hybrid film, 37.4 nm thick, was formed.

UV–Vis spectroscopy and CHI660B electrochemical workstation were utilized to calculate the highest occupied molecular orbital (HOMO) and lowest unoccupied molecular orbital (LUMO) of PBD. The PBD solution and its spin-coated film underwent the optical detection.



Observed from UV–Vis absorption spectra in Fig. 2a, the absorption peak λ_{\max} is located at 309 and 332.5 nm as the absorption edge λ_{edge} is in 356 and 374 nm for the PBD film and solution, respectively. Due to $E_g = hc/\lambda_{\text{edge}}$, the band gap E_g of PBD in the form of the film and solution is 3.48 and 3.32 eV, respectively. Cyclic voltammetry (CV) analysis is shown in Fig. 2b, in which the PBD film is measured in the acetonitrile with TBAP (0.1 mol/L). Its onset oxidation potential E_{ox} vs. the Ag/AgCl reference electrode is determined to be 1.58 eV. HOMO and LUMO can be expressed as follows:

$$E_{\text{HOMO}} = -(E_{\text{ox}}(\text{onset}) + 4.8 - E_{\text{FOC}}) \quad (1)$$

$$E_{\text{LUMO}} = E_{\text{HOMO}} + E_g \quad (2)$$

where the reference energy level of ferrocene (FOC) is 4.8 eV, the external standard potential of the ferrocene/ferrocenium ion couple E_{FOC} vs. the Ag/AgCl reference electrode is 0.43 eV measured by CV. E_{HOMO} (−5.95 eV) and E_{LUMO} (−2.47 eV) can be figured out, whose distribution is depicted in inset of Fig. 2b. JEM-2100 transmission electron microscopy (TEM) was adopted to characterize the surface of the PBD:PMMA(1:1) nanocomposite film in Fig. 2c, d, from which the PBD in the PBD:PMMA(1:1) film presents zonal distribution. Thus,

the energy band diagram of ITO/PBD:PMMA/Al can be described in Fig. 2e.

2-(4-tert-butylphenyl)-5-(4-biphenyl)-1,3,4-oxadiazole, as a kind of electron-transport and hole-blocking material, was used to fabricate ORRAM, inserted between ITO and Al electrodes. I – V characteristics of the resistive switching ITO/PBD/Al were measured by KEITHLEY 4200-SCS semiconductor characterization system, for which the compliance current was restrained to 0.1 A, as indicated in Fig. 3. For starters, the scanning depicts the OFF-state. The steep current change pops up when the device was swept up to $V_{\text{SET}} = 1.6$ V. Transferring from turn-off to turn-on, it is denoted as the write process. The following scanning is attributed to the nonvolatile storage that manifests the “read” process. With the resistive switching reverse-biased, the sample shifts from ON-state to OFF-state when the voltage goes down to $V_{\text{RESET}} = -4.2$ V. It is the erase process with the negative differential resistive characteristic. All of the experiments above perform the procedure “write-read-erase-read”, which conforms the ITO/PBD/Al has ability in bistable I – V characteristics, and the threshold voltage is 1.6 V. The current proportion of the low resistive state (LRS) to the high resistive state (HRS) witnesses that it can reach 6. 1,3,4-oxadiazole moiety is regarded as electron-transport group, which can

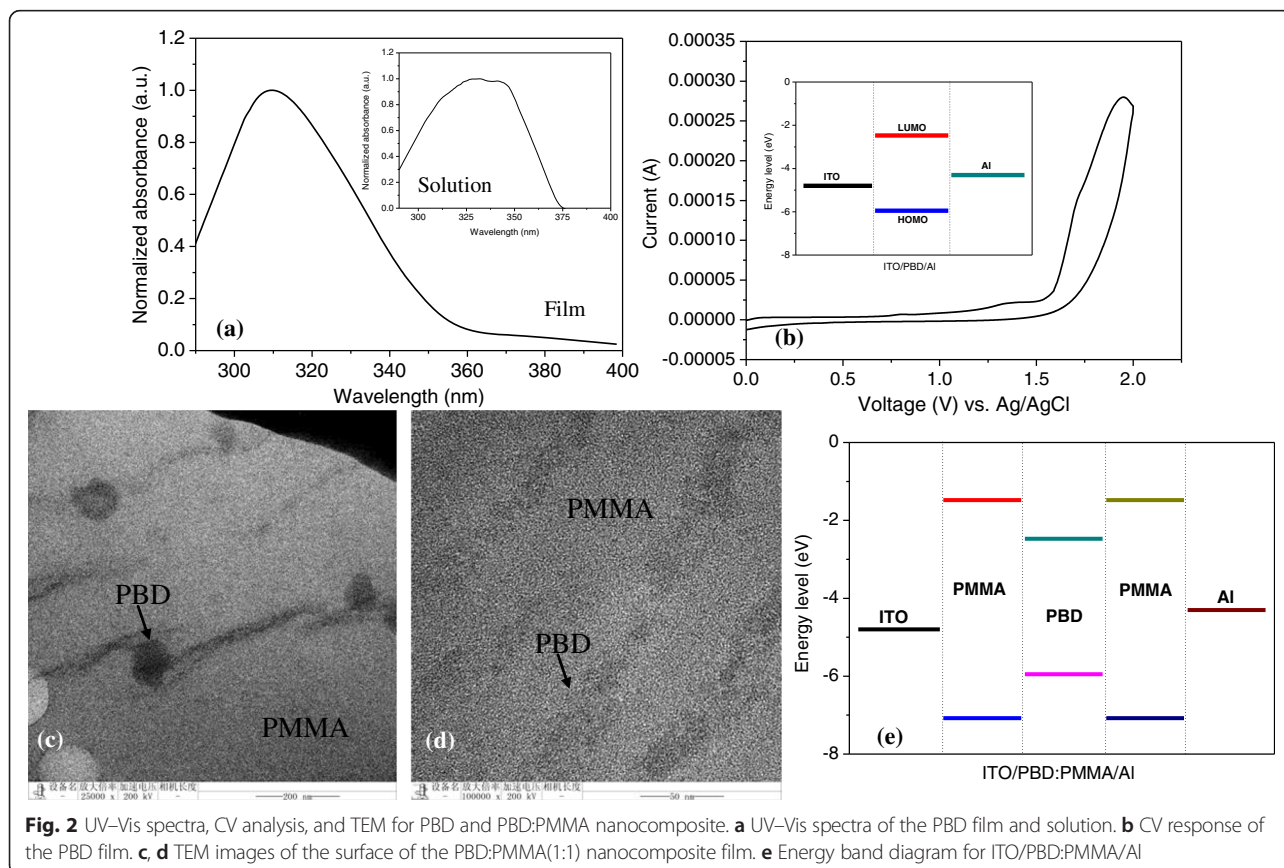
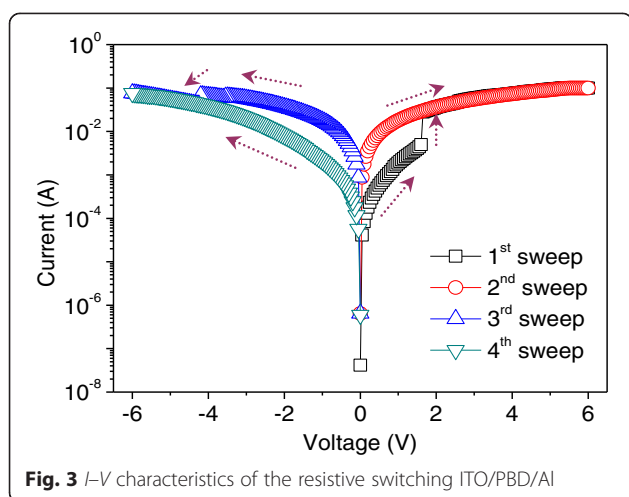


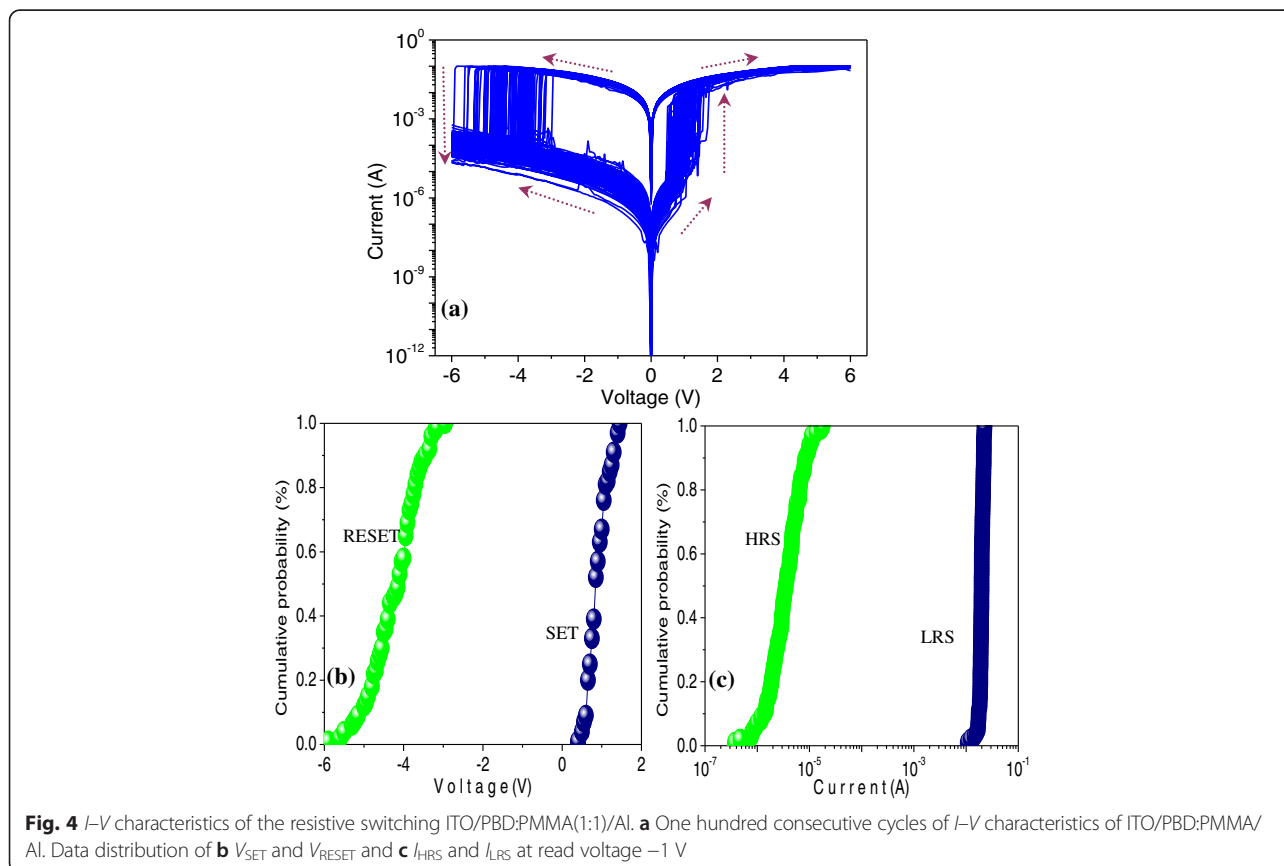
Fig. 2 UV–Vis spectra, CV analysis, and TEM for PBD and PBD:PMMA nanocomposite. **a** UV–Vis spectra of the PBD film and solution. **b** CV response of the PBD film. **c, d** TEM images of the surface of the PBD:PMMA(1:1) nanocomposite film. **e** Energy band diagram for ITO/PBD:PMMA/Al



trap and stabilize electrons [10, 12]. The trap/detrapping mechanism can be responsible for the bistable I - V characteristics of ITO/PBD/Al. At positive bias, the injected electrons occupy the charge traps of the PBD film, leading to the current change of ITO/PBD/Al from OFF-state to ON-state when the traps in the organic material are filled with electrons. The electrons are detrapped from the charge-trapping sites and move to the Al electrode under

reverse bias, where the rupture of the conductive path contributes to the turn-off of the resistive switching.

Polymer nanocomposites are able to exert an exceptional influence on nanoelements in a long-term stability, specifically, to enhance the ON/OFF current ratio of the bistable resistive switching. Thus, PBD:PMMA nanocomposite can be treated as an organic storage material for bistably electrical performance. One hundred consecutive cycles of I - V characteristics for ITO/PBD:PMMA(1:1)/Al were carried out and plotted in Fig. 4a. The cumulative distribution of V_{SET} and V_{RESET} is displayed in Fig. 4b, where the mean (standard deviation) of V_{SET} and V_{RESET} is 0.92 (0.26) V and -4.22 (0.62) V, respectively. At read voltage -1 V, the statistical analysis of ITO/PBD:PMMA(1:1)/Al indicated in Fig. 4c illustrates that the mean (standard deviation) of I_{HRS} and I_{LRS} is 4.47 (3.31) μA and 19.73 (1.90) mA, respectively. Therefore, the resistive switching ITO/PBD:PMMA(1:1)/Al, as same as ITO/PBD/Al, is electrically bistable. Nevertheless, it has a smaller threshold voltage as well as much larger ON/OFF current ratio close to 10^4 . Insulator-like PMMA has higher E_g (approximately 5.6 eV) so that carriers require more energy to inject into the e PBD:PMMA nanocomposite film. The current ratio of the resistive switching for PBD blended with



PMMA is boosted with the fact that the original state of the resistive switching is in higher resistive state. The mechanism of the resistive switching based on PBD:PMMA nanocomposite can be explained by the trap and detrap of electrons in the PBD material. Electrons are injected from the Al electrode to LUMO of PMMA during forward sweep, by means of tunneling mechanism through PMMA molecules [15], which fill the traps of PBD to fulfill the write process at positive bias. During reverse bias, the electrons captured by the trap of PBD are detrapped and released into the PMMA matrix by Fowler-Nordheim tunneling into the Al electrode. Thus, the resistive switching from turn-on to turn-off originates from the rupture of the conductive path that is the erase process of the storage cell.

With regard to the bistability of the resistive switching for ITO/PBD/Al and ITO/PBD:PMMA(1:1)/Al, the conductive mechanism should be further to analyze. Figure 5a, b illustrates “write-read” process and its fitting curves in the logarithmic coordinate. Below 0.3 V, the slope of ITO/PBD/Al and ITO/PBD:PMMA(1:1)/Al is equally identical to 1.0, in line with Ohmic current conduction. Otherwise, the slope of the fitting lines, before the abrupt current transition, is 1.2 and 1.5, respectively. In particular, the slope of the resistive switching ITO/PBD:PMMA(1:1)/Al can reach 2.0 when the sweep increases from 0.9 to 2.0 V. Therefore, space-charge-limited conduction (SCLC) corresponds to I - V characteristics as

the applied bias is above 0.3 V in the write process. During the read process, the current linearly increases with the incremental voltage, in agreement with Ohmic Law. The results above demonstrate the undoped and doped PBD bistable resistive switches are spontaneously adjusted by SCLC and localized filament. For Fowler-Nordheim tunneling mechanism, the tunneling current as an exponential function of $1/V$ is

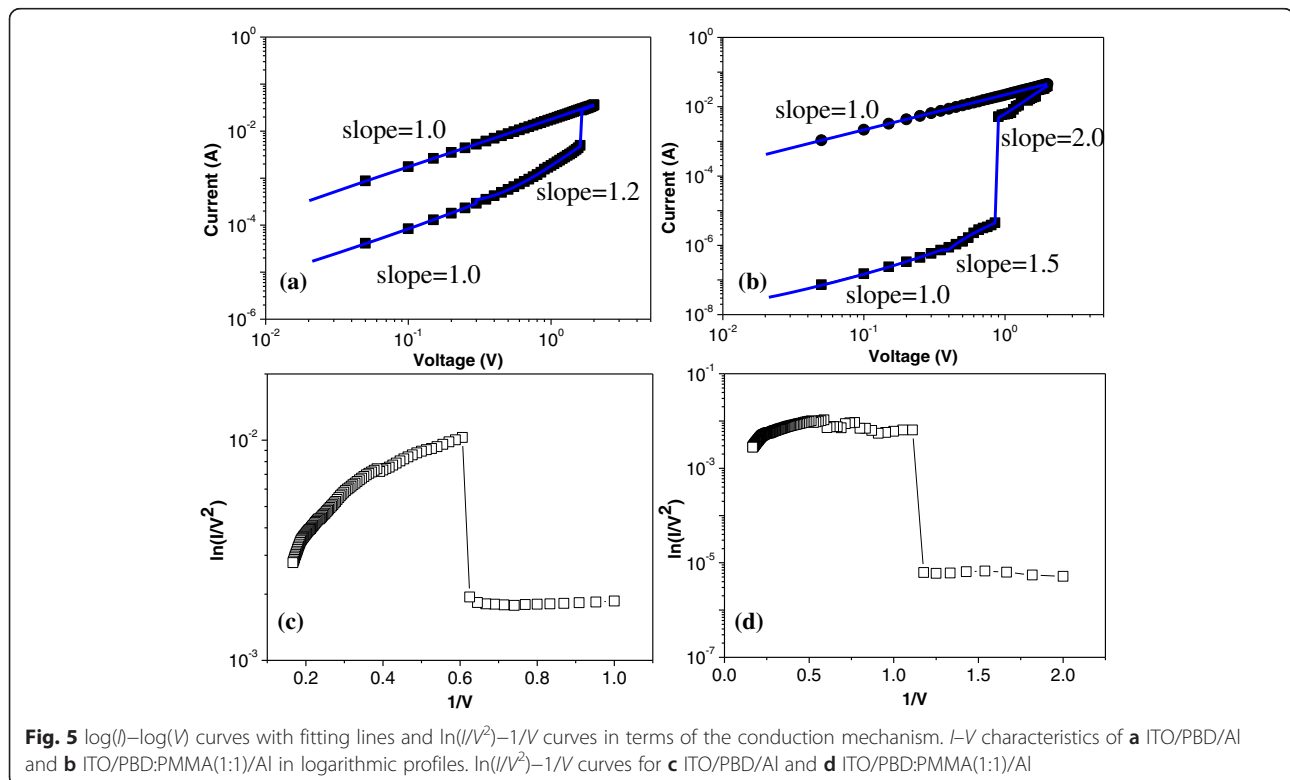
$$I \propto V^2 \exp(-\kappa/V) \quad (3)$$

where κ is the parameter related with the potential barrier shape. If it is a triangular potential barrier,

$$\kappa = 8\pi(2m^*)^{1/2}\phi^{3/2}/3qh \quad (4)$$

where ϕ is the height of the potential barrier, m^* is the efficient mass of holes in the polymer semiconductor, and q and h are the quantity of electric charge and Planck constant, respectively. Depicted in the correlation between $\ln(I/V^2)$ and $1/V$ in Fig. 5c, d, the write process has the negative resistance conduction because the current dramatically increases during the forward scan, consistent with the Fowler-Nordheim (FN) tunneling model.

At ambient temperature, the experimental result in Fig. 6 exhibits the ON-state and OFF-state retention of the nonvolatile resistive switching under constant bias $V = 1$ V and read pulses of 1 V with the period



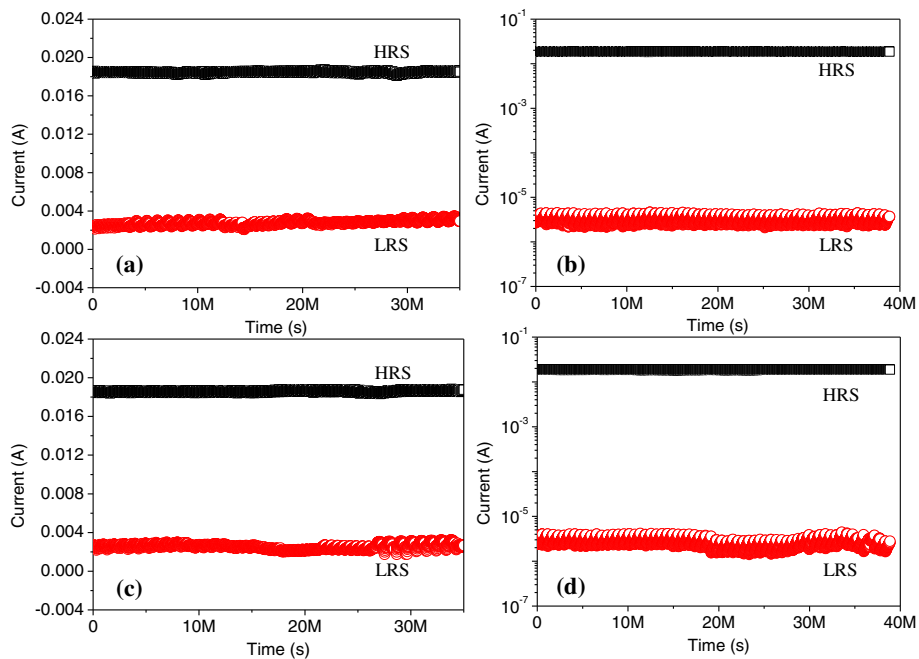


Fig. 6 Data retention of the organic resistive switching and linear fit curves. Retention for **a** ITO/PBD/Al and **b** ITO/PBD:PMMA(1:1)/Al at constant bias and their relative retention performance at read cycles with continuous pulses for **c** ITO/PBD/Al and **d** ITO/PBD:PMMA(1:1)/Al

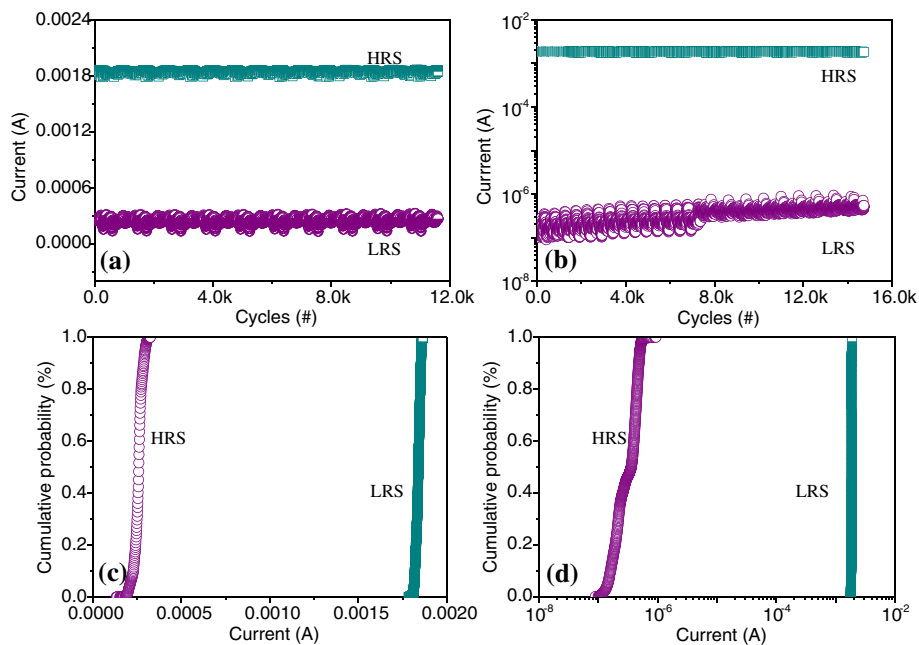


Fig. 7 Endurance cycles and statistical analysis of the bistable resistive switching. Endurance cycles for **a** ITO/PBD/Al and **b** ITO/PBD:PMMA(1:1)/Al. Cumulative probability for **c** ITO/PBD/Al and **d** ITO/PBD:PMMA(1:1)/Al

2 μs and the pulse width 1 μs . Figure 6a, c presents the data retention of the bistable resistive switching ITO/PBD/Al at bias $V=1$ V and read pulses, respectively. In excess of 1-year retention time, the sample, whose ON/OFF current ratio is nearly 6, does not evidently decay. Under the constant voltage and read pulses, the retention of the ITO/PBD:PMMA(1:1)/Al is presented in Fig. 6b, d. With the retention time more than 1 year, this bistable resistive switching in LRS or HRS seems to be more stable and their proportion approaches 10^4 . Aside from that, the bistable switching for ITO/PBD/Al and ITO/PBD:PMMA(1:1)/Al is subject to consecutive endurance cycles ($>10^4$), for which Fig. 7a, b exhibits I_{HRS} and I_{LRS} varying with the cycles at $V_{\text{read}}=0.1$ V. The cumulative distribution of ITO/PBD/Al is displayed in Fig. 7c, where the mean (standard deviation) of I_{HRS} and I_{LRS} is 0.24 (0.05) mA and 1.84 (0.02) mA, respectively. The statistical analysis of ITO/PBD:PMMA(1:1)/Al indicated in Fig. 7d illustrates that the mean (standard deviation) of I_{HRS} and I_{LRS} is 0.37 (0.17) μA and 1.83 (0.02) mA, respectively. It is shown that the resistive switching ITO/PBD:PMMA(1:1)/Al has higher ON/OFF current ratio and better read endurance cycles and retention ability, which results from the wide band-gap of PMMA that holds back the carrier transfer. The reason that the initial resistance of the pristine device is far more than that of ITO/PBD/Al leads to the enhanced memory ability, such as ON/OFF current ratio and retention.

Conclusions

This paper weighs the electrical properties of the undoped and doped PBD films. Although the components of this nanocomposite PBD:PMMA are relatively independent, its performance does not simply add up with the fact that the ON/OFF current ratio is subject to significant enhancement. The bistable behavior of the resistive switching by means of blending PMMA obviously heightens that of the PBD film, which has higher ON/OFF current ratio, and better retention and endurance performance, with the proportionality of the chemical component PBD:PMMA(1:1). Consequently, it provides a widespread prospect for the application of nonvolatile memories.

Competing Interests

The authors declare that they have no competing interests.

Authors' Contributions

LL carried out the experiments, participated in the sequence alignment, and drafted the manuscript. YMS performed the statistical analysis. CPA fulfilled the SEM characterization and measured the nanofilms thickness. JGL participated in the statistical analysis. DZW and XDB conceived the nonvolatile resistive switching based on the organic small molecule and supervised the work. All authors read and approved the final manuscript.

Acknowledgements

This work has been supported by China Postdoctoral Science Foundation (2011 M500701), the National Science Foundation of China (61204127, 21372067), and the Doctoral Fund of Ministry of Education of China (20132301110001).

Received: 18 October 2015 Accepted: 10 November 2015

Published online: 16 November 2015

References

- Jagan SM, Simon MS, Umesh C, Tseung YT (2014) Overview of emerging nonvolatile memory technologies. *Nanoscale Res Lett* 9:526
- Jian TL, Ai WT, Xu L, Ya PC, Miao W, Yu N, Long FL, Qi PL, Yun ZL, Yu FH, Yan BH, Feng T (2014) Negative differential resistance and carrier transport of electrically bistable devices based on poly(N-vinylcarbazole)-silver sulfide composites. *Nanoscale Res Lett* 9:128
- Byungjin C, Sunghun S, Yongsung J, Tae-Wook K, Takhee L (2011) Organic resistive memory devices: performance enhancement, integration, and advanced architectures. *Adv Funct Mater* 21:2806
- Yan MS, Lei L, Dian ZW, Xu DB, Gang L (2015) Bistable electrical switching and nonvolatile memory effect in carbon nanotube-poly(3,4-ethylenedioxythiophene): poly(styrenesulfonate) composite films. *Phys Chem Chem Phys* 17:17150
- Guo MW, Shi BL, Zhao AY, Mei YZ, Yang L, Ding LX, Hang BL, Qi L, Xiao BY, Ming W, Xiao XX, Hong TL, Bao HY, Ming L (2015) Impact of program/erase operation on the performances of oxide-based resistive switching memory. *Nanoscale Res Lett* 10:39
- Debanjan J, Sourav R, Rajeswar P, Mrinmoy D, Sheikh ZR, Rajat M, Siddheswar M (2015) Conductive-bridging random access memory: challenges and opportunity for 3D architecture. *Nanoscale Res Lett* 10:188
- Dian ZW, Xiao HB: Nanostructure quick-switch memristor and method of manufacturing the same. 2013, US Pat 8 487 294 B2.
- Dian ZW, Xiao HB: Method of manufacturing nanostructure quick-switch memristor. 2013, US Pat 8 609 459 B2.
- De WZ, Zheng X, Fu JZ, Shu FS, Su LZ, Yong W, Guang CY, Yan FZ, Hong HX (2007) The effect of electric field strength on electroplex emission at the interface of NPB/PBD organic light-emitting diodes. *Appl Surf Sci* 253:4025
- Yi KF, Cheng LL, Wen CC (2011) New random copolymers with pendant carbazole donor and 1,3,4-oxadiazole acceptor for high performance memory device applications. *J Mater Chem* 21:4778
- Wonsang K, Byungcheol A, Dong MK, Yong GK, Suk GH, Youngkyoo K, Hwajeong K, Moonhor R (2011) Morphology-dependent electrical memory characteristics of a well-defined brush polymer bearing oxadiazole-based mesogens. *J Phys Chem C* 115:19355
- Kyungtae K, Yi KF, Wonsang K, Seungmoon P, Wen CC, Moonhor R (2013) Tunable electrical memory characteristics of brush copolymers bearing electron donor and acceptor moieties. *J Mater Chem C* 1:4858
- Dong YY, Tae WK, Sang WK (2013) Effect of the ZnS shell layer on the charge storage capabilities of organic bistable memory devices fabricated utilizing CuInS₂-ZnS core-shell quantum dots embedded in a poly(methylmethacrylate) layer. *Thin Solid Films* 544:433
- Bipul B, Avijit C, Manik KS, Manisree M, Biswanath M (2013) Electric field induced tunable bistable conductance switching and the memory effect of thiol capped CdS quantum dots embedded in poly(methyl methacrylate) thin films. *J Mater Chem C* 1:1211
- Ramana CHW, Moodely MK, Kannan V, Maity A, Jayaramudu J, Clarke W (2012) Fabrication of stable low voltage organic bistable memory device. *Sensors and Actuators B* 161:684
- Bipul B, Avijit C, Biswanath M (2013) Tuning of electrical conductivity and hysteresis effect in poly(methyl methacrylate)-carbon nanotube composite films. *RSC Adv* 3:3325
- Chao XW, Fu SL, Tai LG (2014) Formation and carrier transport properties of single-layer grapheme/poly(methyl methacrylate) nanocomposite for resistive memory application. *Vacuum* 101:246
- Xiao MW, Wei GX, Jian BX (2014) Graphene based nonvolatile memory devices. *Adv Mater* 26:5496
- Shengli Q, Hiroki I, Lili L, Stephan I, Wenping H, Eiji Y (2013) Electrical switching behavior of a [60] fullerene-based molecular wire encapsulated in a syndiotactic poly(methacrylate) Helical cavity. *Angew Chem* 125:1083

20. Min HL, Jae HJ, Jae HS, Tae WK (2011) Electrical bistabilities and stabilities of organic bistable devices fabricated utilizing [6,6]-phenyl-C85 butyric acid methyl ester blended into a polymethyl methacrylate layer. *Org Electron* 12:1341
21. Hanju J, Jieun K, Jung AL, Hye JC, Youn SK (2013) Organic nonvolatile resistive switching memory based on molecularly entrapped fullerene derivative within a diblock copolymer nanostructure. *Macromol Rapid Commun* 34:355

Submit your manuscript to a SpringerOpen[®] journal and benefit from:

- ▶ Convenient online submission
- ▶ Rigorous peer review
- ▶ Immediate publication on acceptance
- ▶ Open access: articles freely available online
- ▶ High visibility within the field
- ▶ Retaining the copyright to your article

Submit your next manuscript at ▶ springeropen.com
